We are IntechOpen, the world's leading publisher of Open Access books Built by scientists, for scientists

6,900
Open access books available

185,000
International authors and editors

200M
Downloads

Our authors are among the

154
Countries delivered to

TOP 1%
most cited scientists

12.2%
Contributors from top 500 universities



WEB OF SCIENCE™

Selection of our books indexed in the Book Citation Index in Web of Science™ Core Collection (BKCI)

Interested in publishing with us?
Contact book.department@intechopen.com

Numbers displayed above are based on latest data collected.
For more information visit www.intechopen.com



Chapter

Special Crater Types on Vesta and Ceres as Revealed by Dawn

Katrin Krohn

Abstract

The exploration of two small planetary bodies by the Dawn mission revealed multifaced surfaces showing a diverse geology and surface features. Impact crater are the most distinctive features on these planetary bodies. The surfaces of asteroid Vesta and the dwarf planet Ceres reveal craters with an individual appearance as caused by different formation processes. Special topographic and subsurface conditions on both bodies have led to the development of special crater types. This chapter present the three most characteristic crater forms fund on both bodies. Asymmetric craters are found on both bodies, whereas ring-mold craters and floor-fractured craters are only visible on Ceres.

Keywords: asteroids, asymmetric craters, ring mold craters, floor-fractured craters, impact into ice

1. Introduction

The Dawn Mission was the first mission exploring two different planetary objects in the asteroid belt between Mars and Jupiter, the asteroid Vesta and the dwarf planet Ceres. Asteroid Vesta is the second most massive asteroid (2.59079 x 10^{20} kg) with a mean diameter of 525 km and a mean density of 3.456 ± 0.035 g/cm (e.g., [1, 2]). Vesta is believed to be a dry, differentiated proto-planet with an iron core of about 220 km in diameter, a mantle with diogenite compositions and an igneous crust [1, 3, 4]. Asteroid Vesta is a fully differentiated planetary body with a complex topography [2] and a multifaceted morphology including impact basins, various forms of impact craters, large troughs extending around the equatorial region, enigmatic dark material, mass wasting features and surface alteration processes [2, 5, 6]. Vesta's topography reveals extreme height differences resulting in steep slopes, locally exceeding 40° [2, 7, 8]. Those steep slopes result in craters with an unusual asymmetrical shape, where a sharp crater rim exists on the uphill side, and a subdued rim on the downhill side [7]. Impact craters on Vesta range from fresh to highly degraded, suggesting an intensive cratering history [2, 5] similar to the Moon. Vesta is believed to be the host body of HED meteorites (Howardite-Eucrite-Diogenite) (e.g., [9, 10]). The vestan surface is mainly composed of Howardite material with localized enrichments of Eucrite and Diogenite [11, 12]. The surface material consists of thick (100 meters to a few kilometers), multilayered sheets of regolith with different albedos, formed by the accumulation of ejecta from numerous impacts that have resurfaced Vesta over time [2, 13].

The dwarf planet Ceres is the largest object in the asteroid belt with a diameter of 940 km, a mean density of 2.162 ± 0.008 g/cm and a mass of 9.3835 x 10^{20} kg. Ceres is

the only dwarf planet in the inner Solar System, which is supposed to be a relict ocean world [14, 15]. Recent observations by Dawn suggest that Ceres is a weakly differentiated body with a 40 km thick volatile-dominated crust and a rocky mantle down to a depth of 100 km comprising remnants of brines and hydrated rocks such as clays [16]. The crust is thought to be dominated by a mixture of ammoniated phyllosilicates, carbonates, salts, clathrate hydrates and no more than 30–40% water ice [17–20]. This volatile-rich outer layer is suggested to have an average thickness of 41.0 km [21–23]. The brines within the mantle of Ceres could be related to residual liquid from the freezing of a global ocean, as already proposed prior to the Dawn mission [24]. Several locations on Ceres's crust are enriched in salt compounds such as carbonates and ammonium chlorides [25]. A very large amount of the water could exist in the form of clathrate hydrates, which is conforming to geophysical conclusions for the abundance of water in Ceres's crust [17, 20, 26]. Since Ceres's globally homogenous surface is supposed to be made of material formed deep inside, a large-scale formation mechanism is suggested for that scenario. However, local heterogeneities associated with impact craters and landslides containing sodium carbonate and other salts suggest that those components are available in the shallow subsurface [26]. Sodium carbonates are found in brines of two remarkable emplacements on Ceres: Ahuna Mons [27, 28] and the bright (faculae) material in Occator crater (e.g., [19, 29]). Recent emplacement of bright deposits sourced from brines confirms that Ceres is a persistently geologically active world [19]. Generally, sodium carbonates are related to large impacts that can source deep material [26]. The most distinctive features found on both bodies are impact craters. Cratering processes on planetary bodies happen continuously and cause the formation of a large variety of impact crater morphologies. Images from the Dawn Spacecraft have revealed a diversity of impact craters, including craters with an individual appearance. The shape of an impact crater, and mainly its ejecta distribution, is the effect of a multifaceted interaction of topographic setting [30]. The majority of impact craters are more or less symmetrical and circular in shape. They display a classical circular bowl-shaped form with crater rims on the same elevation level at every azimuth and approximately parabolic interior profiles. Special topographic and subsurface conditions on both bodies have led to the development of special crater types. This chapter covers these special crater types found on Vesta and Ceres.

2. Asymmetric craters on Vesta and Ceres

A special type of craters occurs von Vesta. These craters show an asymmetric interior morphology and ejecta distribution and are formed on slopes. The main characteristics are a well-formed semi-circular sharp rim on the uphill side and a smooth rim on the downhill side [2, 7]. The downhill rim is covered by a local accumulation of material, whereas ejected material around the uphill rim is only sporadically distributed in thin layers (**Figure 1**). Mass wasting material is observed on the upslope inner crater walls of most craters. The majority of asymmetric craters have relatively steep inner slope angles of ~24° to 28° on the uphill side and a shallower slope angle of about 13° to 16° on the downhill side [7]. In many cases a straight line occurs on the crater floor between the oblique and the shallow side of the crater at which mass wasting material from the uphill crater wall meets the downhill crater rim material (**Figure 1**). The morphology of asymmetric craters comprises the main type described above (**Figure 1A**), as well as crater with an elongated shape in uphill direction (**Figure 1B**), v-shaped craters with one extended wall (**Figure 1C**) and craters with a lateral elongated form (**Figure 1D**) [7].

Asymmetric craters on Vesta ranging in diameter from 0.3 km to 43 km and are globally distributed. Most craters were formed on slope angles between 10° and 20°.

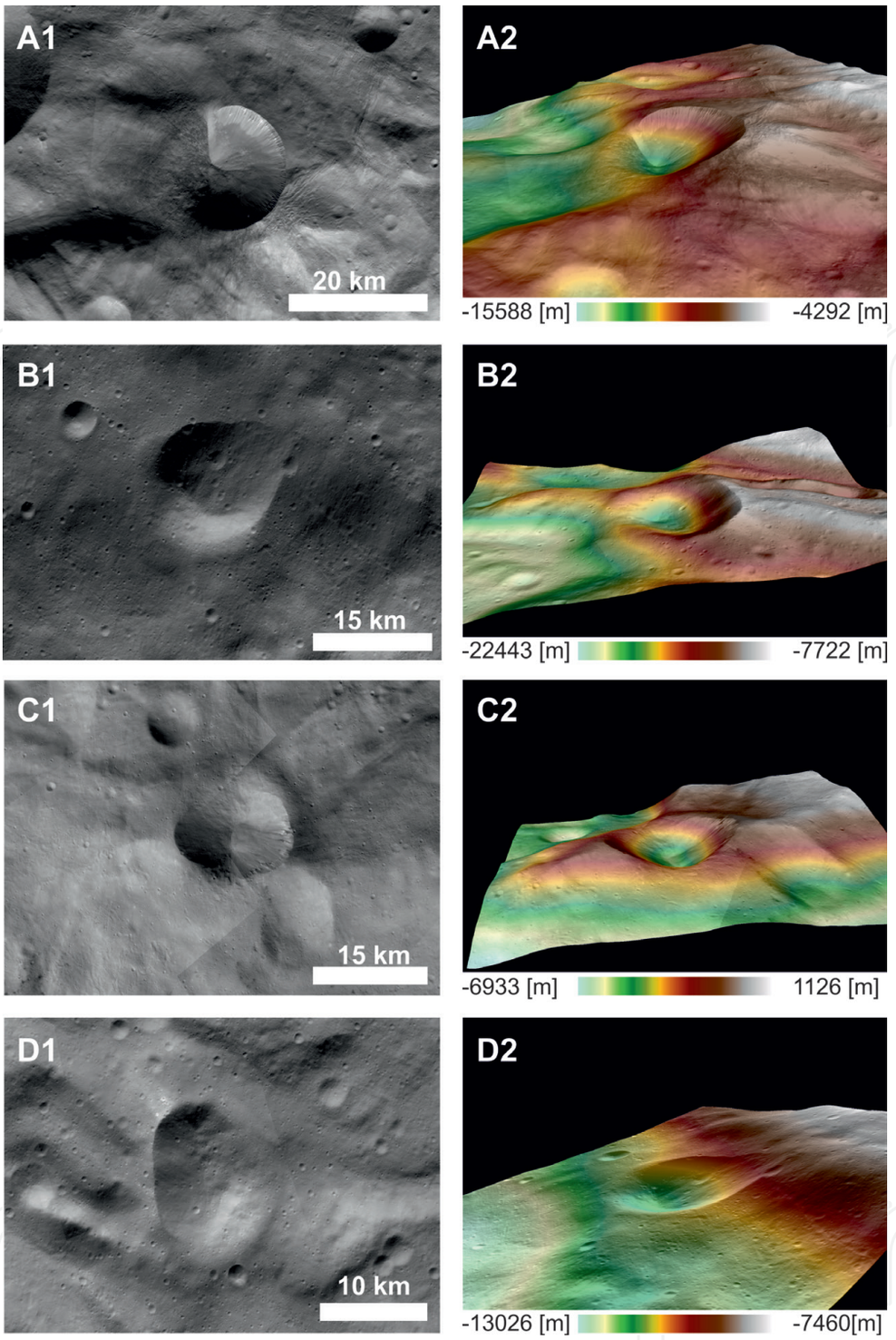


Figure 1.
Examples of asymmetric craters on Vesta. A1 Antonia crater shows the classic type with a smooth downhill rim and a sharp uphill rim which is separated by a straight boundary. B1 oblique elongated crater at 6°S, 299°E. the ejecta is distributed only on the downhill rim. C1 V-shaped crater at 48°S, 129°E. D1 lateral elongated crater at 50°S, long 266°Ewith a downhill ejecta distribution at 501S, long 2661E. A2, B2, C2, D2 show the perspective view of the repective craters.

The authors of [7] shows that the topography is the main cause for the asymmetries observed in these craters on Vesta. Numerical simulations demonstrate that the asymmetric form of these craters can be produced by an oblique impact into a slope. Additionally, the deposition of ejected material in uphill direction is prevented by the slopes, in particular by slopes >20° and results in a larger accumulation of ejecta within the crater and on the downhill crater rim. Post-impact processes are not likely because of comparable ages of crater floors and continuous ejecta [7].

Asymmetric craters are also found on Ceres. The analysis of high resolution data reveals craters similar to those on Vesta, however, with diameters from 0.30 to 4.2 km and a mean of 0.98 km the craters are much smaller [31]. The morphology of those craters shows an asymmetric crater interior with an oblique and a shallower side, as well as an asymmetric ejecta distribution. The crater reveals a semi-circular sharp and well-formed rim on the uphill side, as well as a smooth rim on the downhill side (**Figure 2**). The latter is not clearly detectable because of local accumulation of material covering the downhill crater rim [31].

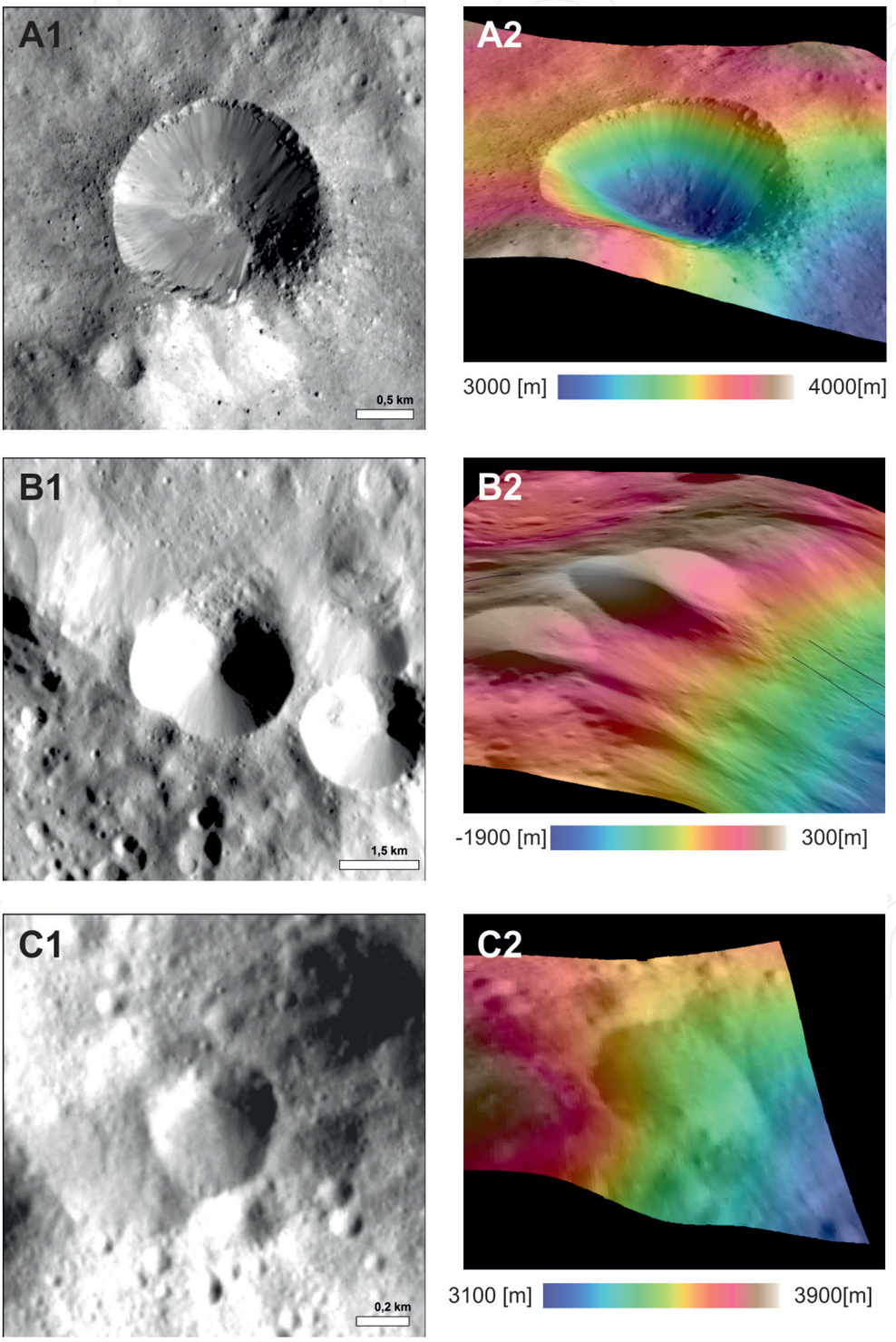


Figure 2.
Examples of asymmetric craters on Ceres. A1 crater at 245.96° E and 12.57° N and B1 crater at 218.18° E and 9.55° S show a sharp uphill rim and a smooth downhill rim, covered withmass wasting material from the crater flanks. C1 crater at 245.16° E and 12.63° N shows a more elongated shape in the uphill direction than the other craters. A2, B2, C2 show the perspective view of the repective craters.

Further similarities to Vesta's asymmetric craters comprise sporadically detected thin layers of ejecta on the uphill rim and mass wasting features on the uphill inner crater wall on most craters. Additionally, a relative straight border in the lower third through the crater, separating the oblique from the shallower crater floor [31]. Asymmetric craters are more or less circular in shape (**Figure 2A**), nevertheless there are craters showing a slightly elongated shape in uphill direction (**Figure 2C**). This crater rim seems to merge with the slope and the downhill rim is less elevated than of the typical asymmetric craters, but with the same ejecta and mass wasting material distribution. The crater floor appears wider than the others. The morphology of these craters indicating a formation on a slope crest [31]. The craters are only visible in high resolution data of the second extended mission of Dawn, and therefore, the study area is limited, although the craters are more or less homogeneous distributed over the study area, spanning around 60° N to 60° S latitude and 197° E to 265° E longitude. Most asymmetric craters are formed on slope angles between 10 and 20 degrees. [31] suggests, that the uphill and downhill material of ejecta were deposited simultaneously, and thus, not influenced by post-emplacement modifications.

Furthermore, the shape and the ejecta distribution as well as the formation on slopes are quite similar to those on Vesta. Although, the crater sizes on Ceres are much smaller for asymmetric craters, the topography is suggested to be the main cause for the asymmetries [31]. Vesta's extreme topographic differences with a total relief of ~41 km [2] have caused many craters to be formed on slopes. Moreover, the topographic differences with a total relief of ~15 on Ceres [23] is less distinctive and not as steep as on Vesta. Thus, the low variations of the topography cause lower slope angles and could have limited the crater size formation on the slopes [31].

3. Ring-mold craters on Ceres

Ring- mold craters (RMC) are common on lineated and lobated debris aprons, filling valleys, and concentric crater fills on Mars [32–34]. They are interpreted as impacts into ice covered by a thin layer of regolith. Ring-mold craters have diameters between 167 and 697 m and are generally surrounded by a rimless, circular moat. Furthermore, ring-mold craters show a variety of complex interior features. [33] found four morphological types of ring-mold craters: (1) a central pit or bowl; (2) a central plateau; (3) a multiring; and (4) central mound craters.

On Ceres ring-mold craters are located on the southern crater floor of Occator [35]. They predominantly appear on the lobate smooth material; a few craters are found on the terrace material as defined on the geologic maps of [36, 37]. Some ring-mold craters are located on or near the tectonic structure in the southern part of the Occator floor. Ring-mold craters show an almost circular shape seem to be subsiding into the surface, causing less elevated crater rims (**Figure 3**). Numerous ring-mold craters are degraded (**Figure 3**) and contains cracks (**Figure 3D**) or lobate material (**Figure 3E** and **F**). [35] found three classes of ring-mold craters: (1) central pit or bowl craters (**Figure 3A**); (2) central mound craters (**Figure 3B** and **C**); and (3) central plateau craters (**Figure 3B**). They show, that ring-mold craters on Ceres are comparable to those on Mars (e.g., [32, 33, 38]). Both bodies show nearly rimless craters with a circular outer moat and similar interior morphologies, like central pits or bowls, plateaus, and mounds. Moreover, ring-mold craters on both bodies are associated with flow features, lineated valley fills and lobate debris aprons on Mars and lobate materials within Occator on Ceres. The similarities of morphology and location indicate a similar formation process [35]. Although, Martian ring-mold craters with diameters between 697 (mean 225 m; [32]) and 750 m (mean 102 m; [33])

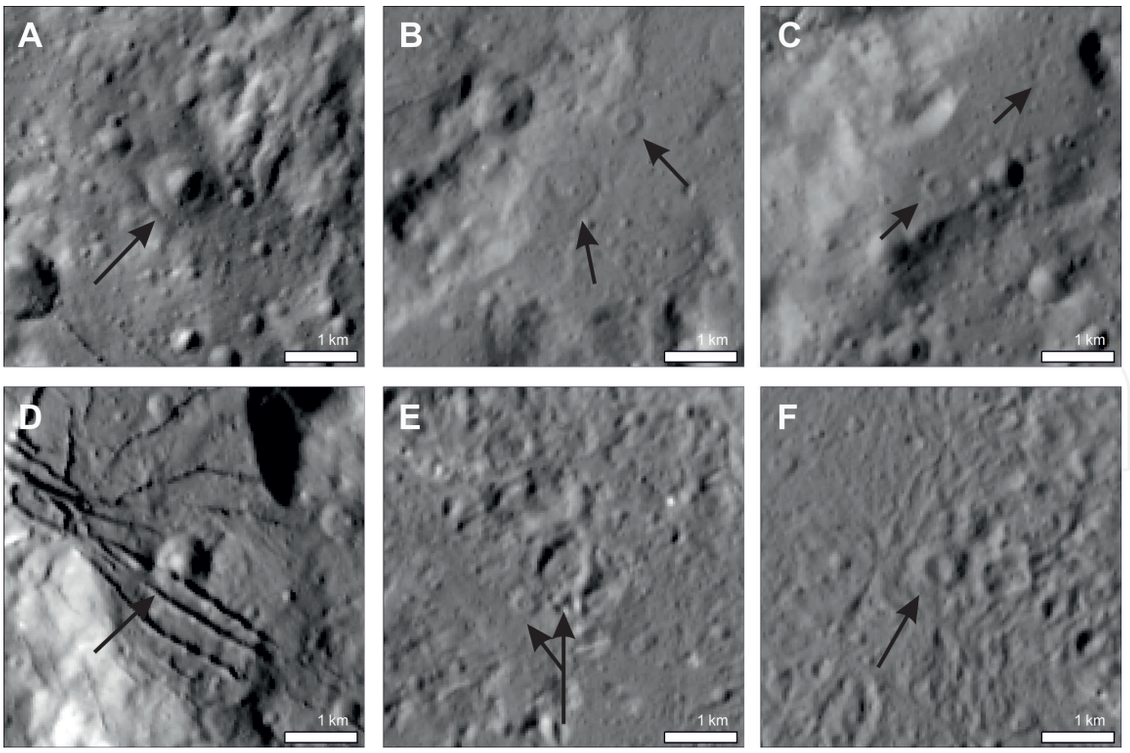


Figure 3.
Ring-mold craters on Ceres. (A) shows a central pit/bowl crater. (B) shows a central plateau (bottom) and a central mound crater (top). (C) shows two central mound craters. (D) shows a ring-mold crater degraded and deformed by cracks. (E) and (F) show craters affected by flow features.

are smaller than ring-mold craters on Ceres with diameters from ~280 to ~1,520 m with a mean of ~710 m [35]. Ponded material and lobate materials within Occator are supposed to be formed by impact melt or cryovolcanic flows (e.g., [39–41]). Furthermore, thermal modeling and gravity data suggest an extensive deep brine reservoir beneath Occator, which might have been mobilized by the heating and deep fracturing related to the Occator impact. Thus, this process would lead to a long-lived extrusion of brines and the formation of the faculae [15]. Additionally, pre-existing tectonic cracks may provide hints for deep brines migrating and dilatating the crust creating a compositional heterogeneity [15].

Due to the occurrence of frozen oceanic materials rich in sodium carbonate and ammonium chloride at several locations, [26] suggest that oceanic material is frozen in the first 10s of kilometers and possibly shallower. This hypothesis is verified by [35] using the depth to diameter ratio from [42] to estimate the minimum regolith thickness on the basis of bowl-shaped craters sizes which are adjacent to ring-mold craters. The results also conclude an overlying area thickness of several tens of meters suggesting that the smaller bowl-shaped crater do not penetrate to the ice layer. Thus, subsurface ice at Occator is at a relatively shallow depth, below a thin protective layer of regolith, and those impacts hitting the subsurface ice layer form ring-mold craters [35].

4. Floor-fractured craters on Ceres

Several impact craters on Ceres contains sets of fractures on their floors. Typical cerean FFCs reveal an irregular shaped rim, which is mostly deformed by slumping or sliding of the crater rim building wall terraces, and/or a central pit or peak structure [43, 44]. The morphology of most fractures is characterized by an irregular pattern with concentric and/or radial or polygonal shape, other fractures are almost

straight and subparallel to parallel [44]. A common fracture structure are crevices merging into various branches or narrow fissures that conjoint into straight wide fractures. These fractures bifurcate into grand fracture groups or networks which can cover nearly half of the crater floor, this is observed at Dantu and Occator crater [44] (**Figure 4A** and **B**). A special type of floor fractures is found within Yalode crater (**Figure 4C**, **C1**). The fractures appear wider and more developed than in other craters and can be divided into two generations. They show high variation in shape, width and lengths and encompass deformational features such as en echelon structures and possible strike slip faults, dilatational jogs or tilted blocks. Such morphologic variations suggest different formation mechanism [44].

The floor-fractures are similar with floor-fractured craters (FFC) of Class 1 and 4 on the Moon (e.g., [43–45]). Depth to diameter ratios show that FFCs on Ceres are anomalously shallow similar to lunar FFCs [43]. Class 1 FFCs on Ceres includes the craters Dantu, Ezinu, Occator, Gaue, Ikapati, Azacca, Haulani, and Kupalo and shows radial and/or concentric fractures on their floors as well as central peaks or pits, similar to Class 1 FFCs on the Moon [43].

In case of Dantu and Occator, the most prominent FFCs on Ceres, an extensive set of crosscutting fractures occur the base of their southern wall (**Figure 4A2**, **B1**). The orientation of most of these fractures is concentric to the base of the crater wall, whereas the fractures at Occator are more concentrated in the southwest corner. Other fractures are orthogonal to and crosscut the concentric ones at both crater floors [43, 44]. Both craters show fractures radial and concentric to the central peak or dome/pit structure, respectively (**Figure 4A1**, **B2**). On Ceres are several linear fractures identified which are related to faculae suggesting a cryovolcanic formation [29, 44, 46, 47]. At Occator the linear fractures are related to the lobate flow fractures of Vinalia Faculae. Dantu shows more crosscutting fractures than Occator, but there are more fractures associated with the central structure [43]. Furthermore,

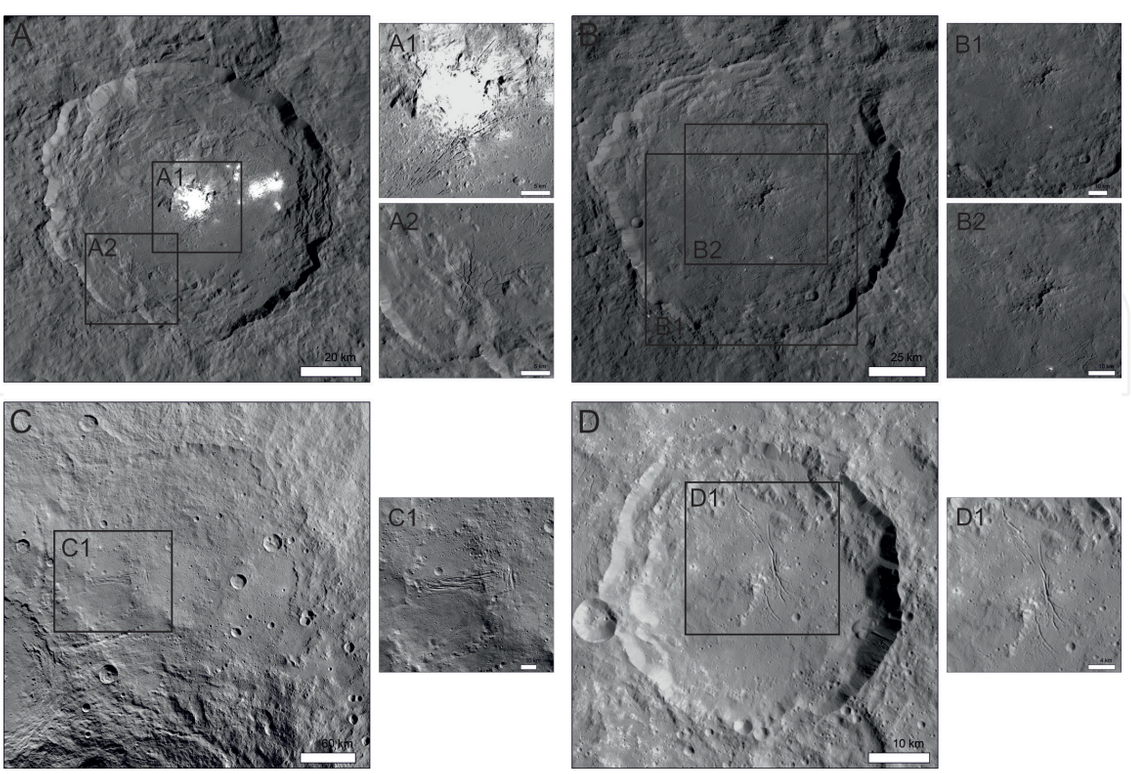


Figure 4.
Examples of FFCs on Ceres. (A) Occator crater and (B) Dantu crater. A1 and B2 shows radial and concentric fractures around the central dome/pit structure. A2 and B1 shows crosscutting fractures at the base of the southern wall, respectively. (C) Yalode crater. C1 shows wider and more developed fractures which can be divided into two generations. (D) Azacca crater. D1 shows curvilinear fractures near the central peak.

in some regions of Occator the space between fractures contains blocky fragments that seem to limit the tear faults. Other fractures are cut by slides [44]. Dantu also shows pitted fractures indicating the influence of volatile components in the subsurface [44].

Other FFCs on Ceres shows a roughly north–south trending set of curvilinear fractures and a smaller set of conjugate fractures associated with the north south fractures near the central peak in the case of Azacca (**Figure 4D**, **D1**), or contains fractures at the base of the northwestern crater wall as well as fractures orthogonal and parallel to the central crater structure in the case of Ikapati [43, 44]. Class 4 FFCs, however, are characterized by having v-shaped moats and usually hummocky floors which are more shallow than other cerean craters of their diameter. The fractures of the crater floors are less distinct. Furthermore, the craters are smaller than Class 1 FFCs [43]. Large FFCs on Ceres with diameters >50 km shows the most similarities with Class 1 lunar FFCs, while smaller FFCs are more consistent with Class 4 lunar FFCs. These results imply a similar formation of fractures due to the intrusion of a low-density material below the craters [43].

The formation of floor fractured craters (FFCs) is mainly suggested by cryomagmatic intrusion [43, 44], at which the cryomagmatic intrusion must have been trapped vertically and horizontally by weak material below the crater. Underlying reservoirs can feed such an intrusion and forming domes which uplifting and fracturing the overlying, brittle crater floor [43, 44]. Additionally, length, width and strike of the fractures vary for each crater and suggest independent formation mechanisms and imply different surface and subsurface materials. [44] also propose the following formation processes for FFCs: (1) tear-off edges in case of slumping of the crater wall, (2) cooling melting processes that lead to sinkage of the crater floor, (3) degassing, and/or (4) tectonic interactions. All four mechanism also comprises up-doming of material beneath the craters.

5. Conclusions

Even on small bodies impact craters reveal a multifaced morphology as caused by different formation processes. Impacts into a slope can cause the formation of asymmetric craters. Whereas steep slope angles and bigger slope sizes promote the formation of the asymmetries. However, the formation of ring-mold crater and floor-fractured crater is mainly cause by the subsurface conditions. An impact into a thin layer of regolith on top of a subsurface ice-layer lead to the formation of ring-mold crater. The occurrence of ring-mold craters can be used to detect regolith covered ice layers. Furthermore, the maximum depth of associated bowl-shaped craters can be used to estimate the depth of the ice and the thickness of overlying regolith. Floor-fractured craters is mainly proposed by cryomagmatic intrusion, which are fed by underlaying reservoirs. But also tear-off edges in case of slumping of the crater wall, cooling melting processes that lead to sinkage of the crater floor, degassing, and/or tectonic interactions are supposed to promote the formation of these crater types.

Appendices and nomenclature

FFC	Floor-fractured crater
HED	Howardite-Eucrite-Diogenite metroids
RMC	Ring-mold crater
Ahuna Mons	10.48° S, 316.2° E

Antonia crater	58.7° S, 350.78° E
Azacca crater	6.66° S, 218.4° E
Dantu crater	24.3° N, 138.23° E
Ezinu crater	43.24° N, 195.7° E
Gaue crater	30.81° N, 86.16° E
Haulani crater	5.8° N, 10.77° E
Ikapati crater	33.84° N, 45.6° E
Kupalo crater	39.44° S, 173.2° E
Occator crater	19.82° N, 239.33° E
Vinalia Facula	20.2° N, 242° E
Yalode crater	42.58° S, 292.48° E

IntechOpen

IntechOpen

Author details

Katrin Krohn
German Aerospace Center (DLR), Berlin, Germany

*Address all correspondence to: katrin.krohn@dlr.de

IntechOpen

© 2021 The Author(s). Licensee IntechOpen. This chapter is distributed under the terms of the Creative Commons Attribution License (http://creativecommons.org/licenses/by/3.0), which permits unrestricted use, distribution, and reproduction in any medium, provided the original work is properly cited. CC BY

References

[1] Russell CT, Raymond CA, Coradini A, McSween HY, Zuber MT, Nathues A, et al. Dawn at Vesta: Testing the Protoplanetary Paradigm. Science. 2012;336:684-6.

[2] Jaumann R, Williams DA, Buczkowski DL, Yingst RA, Preusker F, Hiesinger H, et al. Vesta's shape and morphology. Science. 2012;336:687-90.

[3] McCord TB, McFadden LA, Russell CT, Sotin C, Thomas PC. Ceres,Vesta, and Pallas: Protoplanets, Not Asteroids. EOS Transactions. 2006;87:105-9.

[4] Keil K. Geological History of Asteroid 4 Vesta: The "Smallest Terrestrial Planet". Asteroids III2002. p. 573.

[5] Schenk P, O'Brien DP, Marchi S, Gaskell R, Preusker F, Roatsch T, et al. The Geologically Recent Giant Impact Basins at Vesta's South Pole. Science. 2012;336:694-7.

[6] Buczkowski DL, Wyrick DY, Iyer KA, Kahn EG, Scully JEC, Nathues A, et al. Large-scale troughs on Vesta: A signature of planetary tectonics. Geophysical Research Letters. 2012;39:18205.

[7] Krohn K, Jaumann R, Elbeshausen D, Kneissl T, Schmedemann N, Wagner R, et al. Asymmetric craters on Vesta: Impact on sloping surfaces. Planetary and Space Science. 2014;103:36-56.

[8] Krohn K, Jaumann R, Otto K, Hoogenboom T, Wagner R, Buczkowski DL, et al. Mass movement on Vesta at steep scarps and crater rims. Icarus. 2014;244:120-32.

[9] McCord TB, Li J-Y, Combe J-P, McSween HY, Jaumann R, Reddy V, et al. Dark material on Vesta from the infall of carbonaceous volatile-rich material. Nature. 2012;491:83-6.

[10] McCord TB, Adams JB, Johnson TVJS. Asteroid Vesta: Spectral Reflectivity and Compositional Implications. 1970;168:1445.

[11] Prettyman TH, Mittlefehldt DW, Yamashita N, Lawrence DJ, Beck AW, Feldman WC, et al. Elemental Mapping by Dawn Reveals Exogenic H in Vesta's Regolith. Science. 2012;338:242-6.

[12] De Sanctis MC, Ammannito E, Capria MT, Tosi F, Capaccioni F, Zambon F, et al. Spectroscopic Characterization of Mineralogy and Its Diversity Across Vesta. Science. 2012;336:697-700.

[13] Jaumann R, Nass A, Otto K, Krohn K, Stephan K, McCord TB, et al. The geological nature of dark material on Vesta and implications for the subsurface structure. Icarus. 2014;240:3-19.

[14] Castillo-Rogez J. Future exploration of Ceres as an ocean world. Nature Astronomy. 2020;4:732.

[15] Raymond CA, Ermakov AI, Castillo-Rogez JC, Marchi S, Johnson BC, Hesse MA, et al. Impact-driven mobilization of deep crustal brines on dwarf planet Ceres. Nature Astronomy. 2020;4:741.

[16] Castillo-Rogez JC, Hesse MA, Formisano M, Sizemore H, Bland M, Ermakov AI, et al. Conditions for the Long-Term Preservation of a Deep Brine Reservoir in Ceres. Geophysical Research Letters. 2019;46(4):1963-72.

[17] Bland MT, Raymond CA, Schenk PM, Fu RR, Kneissl T, Pasckert JH, et al. Composition and structure of the shallow subsurface of Ceres revealed by crater morphology. Nature Geoscience. 2016;9:538-42.

[18] De Sanctis MC, Ammannito E, Raponi A, Marchi S, McCord TB,

McSween HY, et al. Ammoniated phyllosilicates with a likely outer Solar System origin on (1) Ceres. Nature. 2015;528:241-4.

[19] De Sanctis MC, Raponi A, Ammannito E, Ciarniello M, Toplis MJ, McSween HY, et al. Bright carbonate deposits as evidence of aqueous alteration on (1) Ceres. Nature. 2016;536:54-7.

[20] Fu RR, Ermakov AI, Marchi S, Castillo-Rogez JC, Raymond CA, Hager BH, et al. The interior structure of Ceres as revealed by surface topography. Earth and Planetary Science Letters. 2017;476:153-64.

[21] Ermakov AI, Fu RR, Castillo-Rogez JC, Raymond CA, Park RS, Preusker F, et al. Constraints on Ceres' Internal Structure and Evolution From Its Shape and Gravity Measured by the Dawn Spacecraft. Journal of Geophysical Research (Planets). 2017;122:2267-93.

[22] Park RS, Konopliv AS, Bills BG, Rambaux N, Castillo-Rogez JC, Raymond CA, et al. A partially differentiated interior for (1) Ceres deduced from its gravity field and shape. Nature. 2016;537:515-7.

[23] Russell CT, Raymond CA, Ammannito E, Buczkowski DL, De Sanctis MC, Hiesinger H, et al. Dawn arrives at Ceres: Exploration of a small, volatile-rich world. Science. 2016;353:1008-10.

[24] Castillo-Rogez JC, McCord TB. Ceres' evolution and present state constrained by shape data. Icarus. 2010;205:443-59.

[25] de Sanctis MC, Ammannito E, Carrozzo FG, Ciarniello M, Giardino M, Frigeri A, et al. Ceres's global and localized mineralogical composition determined by Dawn's Visible and Infrared Spectrometer (VIR). Meteoritics and Planetary Science. 2018;53:1844-65.

[26] Castillo-Rogez J, Neveu M, McSween HY, Fu RR, Toplis MJ, Prettyman T. Insights into Ceres's evolution from surface composition. Meteorit Planet Sci. 2018;53(9):1820-43.

[27] Ruesch O, Platz T, Schenk P, McFadden LA, Castillo-Rogez JC, Quick LC, et al. Cryovolcanism on Ceres. Science. 2016;353.

[28] Zambon F, Raponi A, Tosi F, De Sanctis MC, McFadden LA, Carrozzo FG, et al. Spectral analysis of Ahuna Mons from Dawn mission's visible-infrared spectrometer. Geophysical Research Letters. 2017;44:97-104.

[29] Ruesch O, Genova A, Neumann W, Quick LC, Castillo-Rogez JC, Raymond CA, et al. Slurry extrusion on Ceres from a convective mud-bearing mantle. Nature Geoscience. 2019;12:505.

[30] Elbeshausen D, Wünnemann K. The Effect of Target Topography and Impact Angle on Crater Formation — Insight from 3D Numerical Modelling. Lunar and Planetary Institute Science Conference Abstracts; March 1, 20112011. p. 1778.

[31] Krohn K, Jaumann R, Wickhusen K, Otto KA, Kersten E, Stephan K, et al. Asymmetric Craters on the Dwarf Planet Ceres—Results of Second Extended Mission Data Analysis. Geosciences. 2019;9:475.

[32] Baker DMH, Head JW, Marchant DR. Flow patterns of lobate debris aprons and lineated valley fill north of Ismeniae Fossae, Mars: Evidence for extensive mid-latitude glaciation in the Late Amazonian. Icarus. 2010;207(1):186-209.

[33] Kress AM, Head JW. Ring-mold craters in lineated valley fill and lobate

debris aprons on Mars: Evidence for subsurface glacial ice. Geophysical Research Letters. 2008;35.

[34] Kress AM, Head JW. Ring-Mold Craters on Lineated Valley Fill, Lobate Debris Aprons, and Concentric Crater Fill on Mars: Implications for Near-Surface Structure, Composition, and Age. Lunar and Planetary Science Conference; March 1, 20092009.

[35] Krohn K, Neesemann A, Jaumann R, Otto KA, Stephan K, Wagner RJ, et al. Ring-Mold Craters on Ceres: Evidence for Shallow Subsurface Water Ice Sources. Geophysical Research Letters. 2018;45(16):8121-8.

[36] Buczkowski DL, Scully JEC, Quick L, Castillo-Rogez J, Schenk PM, Park RS, et al. Tectonic analysis of fracturing associated with occator crater. Icarus. 2019;320:49-59.

[37] Scully JEC, Buczkowski DL, Raymond CA, Bowling T, Williams DA, Neesemann A, et al. Ceres' Occator crater and its faculae explored through geologic mapping. Icarus. 2019;320:7-23.

[38] Pedersen GBM, Head JW. Evidence of widespread degraded Amazonian-aged ice-rich deposits in the transition between Elysium Rise and Utopia Planitia, Mars: Guidelines for the recognition of degraded ice-rich materials. Planetary and Space Science. 2010;58:1953-70.

[39] Krohn K, Jaumann R, Stephan K, Otto KA, Schmedemann N, Wagner RJ, et al. Cryogenic flow features on Ceres: Implications for crater-related cryovolcanism. Geophysical Research Letters. 2016;43:1-10.

[40] Schenk P, Marchi S, O'Brien D, Bland M, Platz T, Hoogenboom T, et al. Impact Cratering on the Small Planets Ceres and Vesta: S-C Transitions, Central Pits, and the Origin of Bright Spots. Lunar and Planetary Science Conference; March 1, 20162016. p. 2697.

[41] Jaumann R, Preusker F, Krohn K, von der Gathen I, Stephan K, Matz K-D, et al. Topography and Geomprphology of the Interior of Occator Crater on Ceres. Lunar and Planetary Science Conference; March 1, 20172017.

[42] Hiesinger H, Marchi S, Schmedemann N, Schenk P, Pasckert JH, Neesemann A, et al. Cratering on Ceres: Implications for its crust and evolution. Science. 2016;353(6303).

[43] Buczkowski DL, Sizemore HG, Bland MT, Scully JEC, Quick LC, Hughson KHG, et al. Floor-Fractured Craters on Ceres and Implications for Interior Processes. Journal of Geophysical Research (Planets). 2018;123:3188-204.

[44] Krohn K, von der Gathen I, Buczkowski DL, Jaumann R, Wickhusen K, Schulzeck F, et al. Fracture geometry and statistics of Ceres' floor fractures. Planetary and Space Science. 2020;187:104955.

[45] Schultz PH. Floor-fractured lunar craters. Moon. 1976;15:241-73.

[46] Buczkowski DL, Williams DA, Scully JEC, Mest SC, Crown DA, Schenk PM, et al. The geology of the occator quadrangle of dwarf planet Ceres: Floor-fractured craters and other geomorphic evidence of cryomagmatism. Icarus. 2017.

[47] Quick LC, Buczkowski DL, Scully JEC, Ruesch O, Castillo-Rogez J, Raymond CA, et al. Thermal and Compositional Evolution of a Brine Reservoir Beneath Ceres' Occator Crater: Implications for Cryovolcanism at the Surface. Lunar and Planetary Science Conference; March 1, 20182018.